Supplementary Methods

Surface immunostaining

For internalization studies, cells were incubated for 30 min at 37°C with a primary monoclonal mouse anti-HA antibody, washed, kept at 37°C for 30, 60, 120, or 180 min to allow internalization of the channel, fixed, and stained with a secondary Alexa488-conjugated antibody to assess the time-dependence of surface expression of the channel. Confocal images were acquired at low magnification with a Zeiss LSM780 microscope and the field fluorescence intensity was analyzed using ImageJ software.

Fluorescence recovery after photobleaching (FRAP)

Fluorescence recovery after photobleaching (FRAP) was performed at 37°C on live tsA-201 cells expressing mCherry-tagged $Ca_v3.2$ channels together with the ER-GFP or Golgi-GFP in order to visualize cell compartments. FRAP was performed using a confocal microscope LSM780 (Zeiss), with a 1.4 aperture 63x oil-immersion objective. The GFP and mCherry fluorescence were excited at 488 nm and 587 nm, respectively, and fluorescence signals were collected using separate bandpass filters. A region of interest (ROI) for photobleaching was chosen and three pre-bleached images were collected at 2% laser intensity, following by photobleaching at 80% laser intensity using 6 iterations. The recovery of fluorescence was recorded at 2% laser intensity. Additionally, the fluorescence of a non-bleached background region was monitored. Images were analyzed using ImageJ software and the Time Series Analyzer plugin as previously described [1,2]. Fluorescence in a given ROI was measured, the background signal was subtracted, and the values were corrected for the non-specific photobleaching in non-bleached ROI. Pre-bleaching fluorescence signals were normalized to 100%, and post-bleaching signals to 0%. The normalized fluorescence recovery was plotted as a function of time.

Supplementary figures

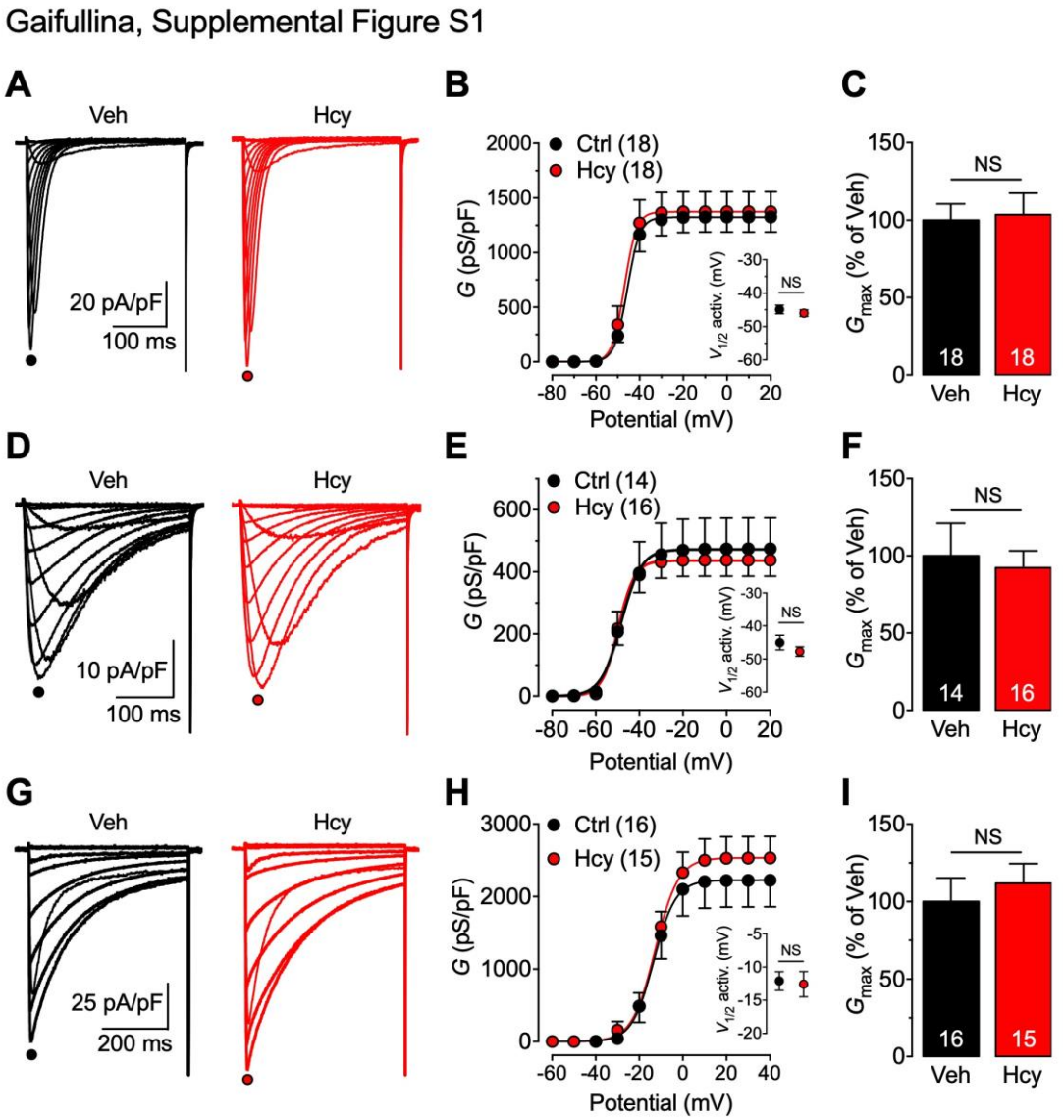

Fig. S1. Effect of homocysteine on recombinant $Ca_V3.1$, $Ca_V3.3$ and $Ca_V2.2$ channels. (A) Representative T-type current traces recorded from $Ca_V3.1$-expressing tsA-201 cells grown in control conditions (black traces) and in the presence of homocysteine (red traces) in response 150 ms depolarizing steps varied from -80 to +40 mV from a holding potential of -100 mV. (B) Corresponding mean conductance/voltage relationships for vehicle-treated (black circles) and homocysteine-treated cells (red circles); the *inset* indicates the corresponding mean half-activation potential. (C) Normalized maximum slope conductance G_{max} for vehicle- (black bar) and homocysteine-treated cells (red bar). (D) Representative T-type current traces recorded from $Ca_V3.3$-expressing tsA-201

cells grown in control condition (black traces) and in the presence of homocysteine (red traces) in response 300 ms depolarizing steps varied from -80 to +40 mV from a holding potential of -100 mV. (E-F) Legend same as for (B-C) but for cells expressing $Ca_v3.3$ channels. (G) Representative N-type current traces recorded from $Ca_v2.2/\alpha_2\delta$-1/β-expressing CHO cells grown in control condition (black traces) and in the presence of homocysteine (red traces) in response 500 ms depolarizing steps varied from -60 to +40 mV from a holding potential of -90 mV. (H-I) Legend same as for (B-C) but for cells expressing $Ca_v2.2/\alpha_2\delta$-1/β.

Gaifullina, Supplemental Figure S2

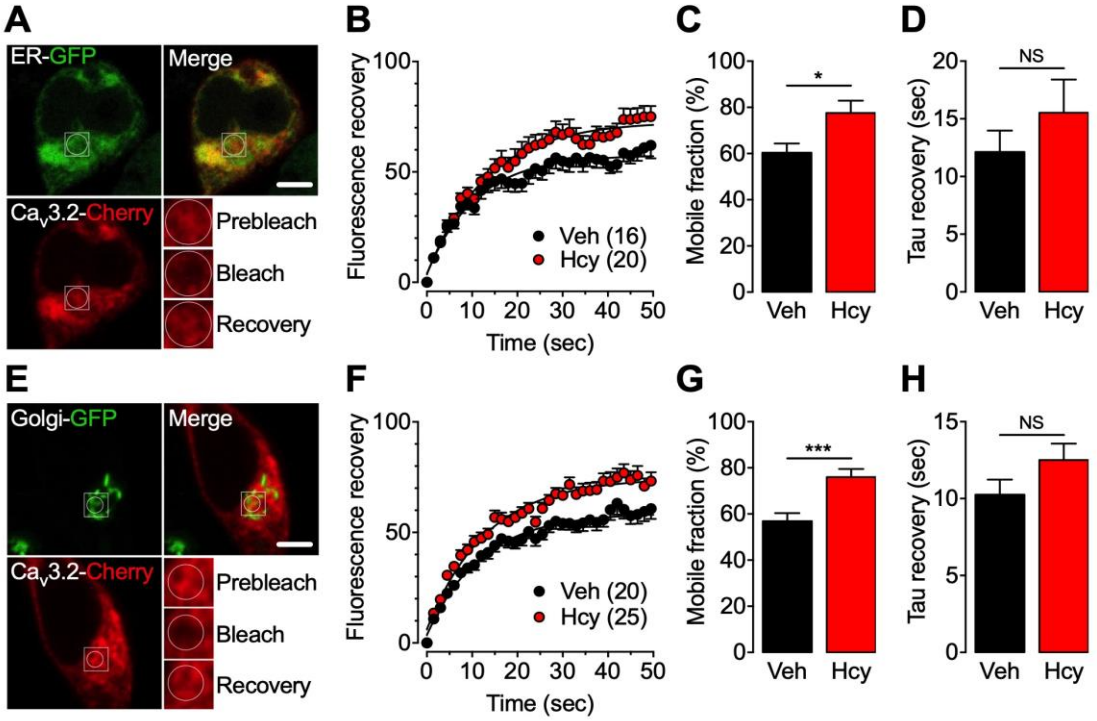

Fig. S2. Effect of homocysteine on the intracellular mobility of $Ca_v3.2$ channels. (A) Representative confocal images of live tsA-201 cells expressing mCherry-tagged $Ca_v3.2$ (red) together with the ER-targeted GFP (green) used for FRAP measurements in the ER. Scale 5 μm. *Insets* show a magnification of the region of interest before (prebleach), immediately after (bleach), and 40 s after photobleaching of mCherry-$Ca_v3.2$ (recovery). (B) Corresponding mean normalized recovery of fluorescence for cells treated with vehicle (black circles) and eHcy (red circles). (C) Corresponding mean mobile fraction of mCherry-$Ca_v3.2$ in vehicle- (black bar) and homocysteine-treated cells (red bar). (D) Corresponding time constant of mCherry-$Ca_v3.2$ fluorescence recovery kinetics in vehicle- (black bar) and eHcy-treated cells (red bar). (E to H) Same as in (A to D) but for cells expressing the Golgi-targeted GFP to assess the mobility of mCherry-$Ca_v3.2$ in the Golgi apparatus.

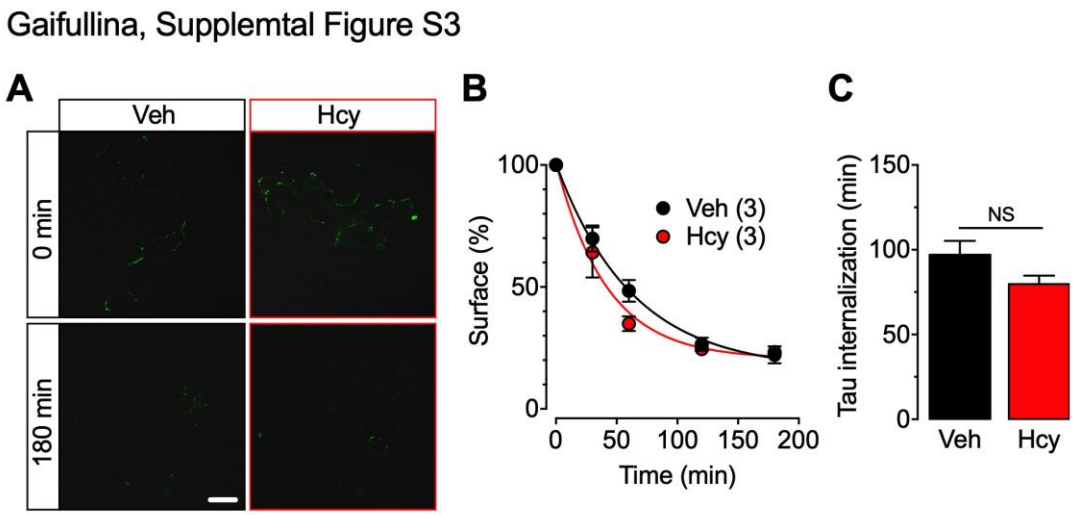

Fig. S3. Effect of homocysteine on internalization of $Ca_v3.2$ channels. (A) Representative confocal images of non-permeabilized tsA-201 cells expressing HA-tagged $Ca_v3.2$ channels and live immunostained with a primary anti-HA antibody before internalization (top panels) and after 180 min internalization (bottom panels) of the channel at 37°C for control cells (left panels) and cells treated with homocysteine (right panels). Scale 20 µm. (B) Corresponding mean internalization kinetics assed by monitoring the time-dependent surface expression of $Ca_v3.2$ channels. Each measurement was obtained by averaging the fluorescence intensity of 10 confocal fields from independent experiments. (C) Corresponding mean time constant values of internalization kinetics.

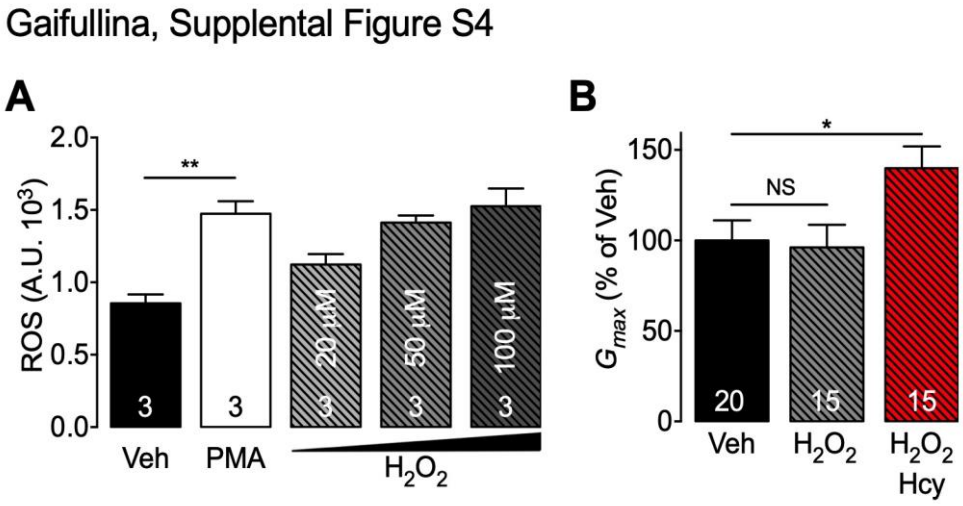

Fig. S4. Effect of ROS production on homocysteine-dependent potentiation of $Ca_V3.2$ channels. (A) Mean ROS production in vehicle (black bar), PMA (white bar), and H_2O_2-treated tsA-201 cells (grey dashed bars) for 24h. (B) Mean normalized maximal T-type conductance for cells expressing $Ca_V3.2$ in control (black bar), H_2O_2 (50 μM) (grey dashed bar), and H_2O_2 + homocysteine conditions (red dashed bar).

Gaifullina, Supplemental Figure 5

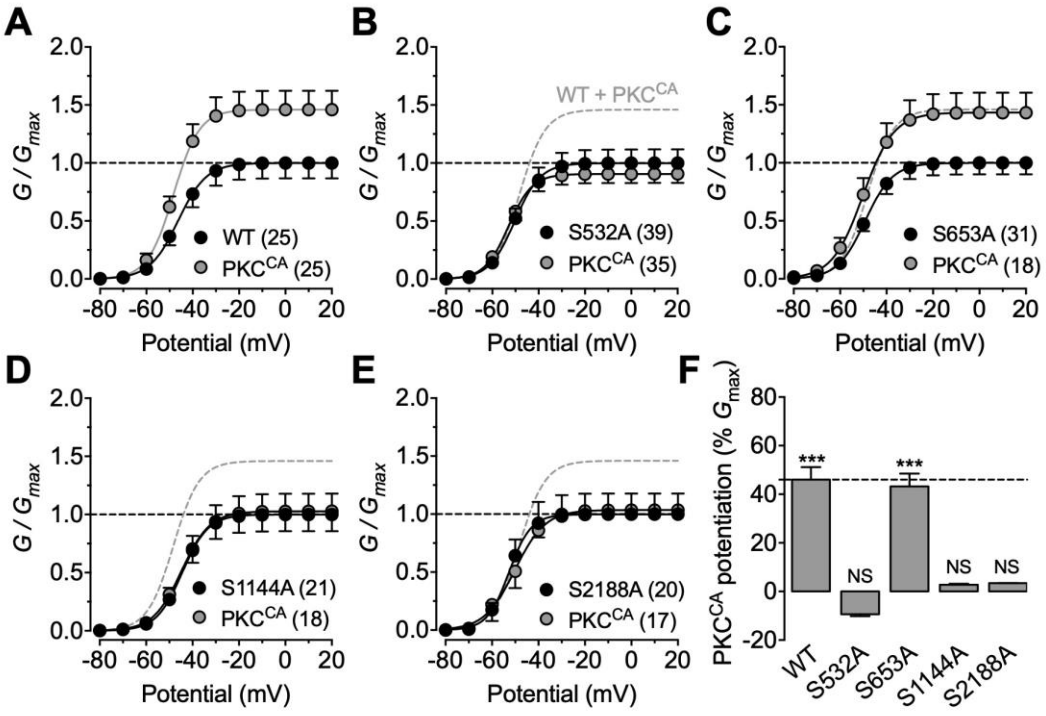

Fig. S5. Effect of PKC on $Ca_v3.2$-deficient PKC phosphorylation. (A to E) Mean normalized macroscopic conductance recorded from cells expressing $Ca_v3.2$ WT (A), S532A (B), S653A (C), S1144A (D), and S2188A mutants (E) alone (black circles) or in combination with the constitutively active mutant of PKC (PKC^{CA}) (grey circles). For comparison, the grey dotted line indicates the conductance values measured for wild-type channels in the presence of PKC^{CA}. (F) Corresponding mean PKC^{CA}-dependent maximal G_{max} potentiation.

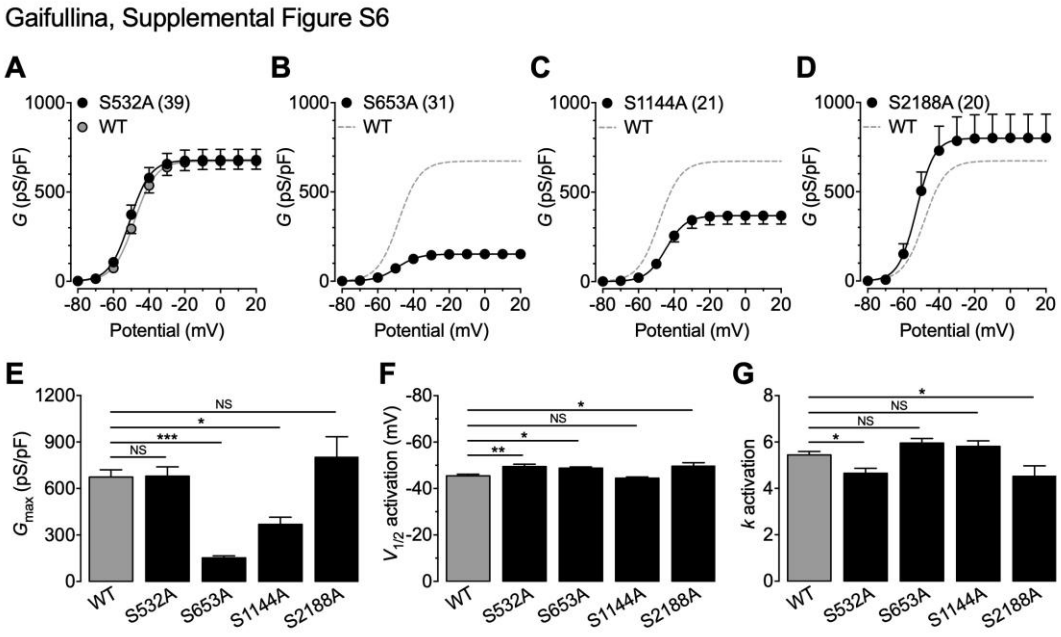

Fig. S6. Expression of phosphorylation-deficient $Ca_v3.2$ mutants. (A to D) Mean macroscopic conductance recorded from tsA-201 cells expressing $Ca_v3.2$ S532A (A), S653A (B), S1144A (C), and S2188A (D) mutants. For comparison, the macroscopic conductance for cells expressing the WT channel is shown (grey). (E) Corresponding mean maximal conductance for WT channels (grey bar) and phosphorylation-deficient mutants (black bars). (F and G) Corresponding mean half-activation potential and activation slope factor, respectively.

References

[1] Hatch AL, Ji WK, Merrill RA, Strack S, Higgs HN. Actin filaments as dynamic reservoirs for Drp1 recruitment. Mol Biol Cell 2016;27:3109-3121.

[2] Logan T, Bendor J, Toupin C, Thorn K, Edwards RH. α-Synuclein promotes dilation of the exocytotic fusion pore. Nat Neurosci 2017;20:681-689.